Eur. Phys. J. C 5, 195–203 (1998)
DOI 10.1007/s100529800901

THE EUROPEAN PHYSICAL JOURNAL C

Measurement of the $B_d^0 - \bar{B}_d^0$ oscillation frequency

The L3 Collaboration

M. Acciarri[27], O. Adriani[16], M. Aguilar-Benitez[26], S. Ahlen[11], J. Alcaraz[26], G. Alemanni[22], J. Allaby[17], A. Aloisio[29], M.G. Alviggi[29], G. Ambrosi[19], H. Anderhub[49], V.P. Andreev[38], T. Angelescu[13], F. Anselmo[9], A. Arefiev[28], T. Azemoon[3], T. Aziz[10], P. Bagnaia[37], L. Baksay[44], R.C. Ball[3], S. Banerjee[10], Sw. Banerjee[10], K. Banicz[46], A. Barczyk[49,47], R. Barillère[17], L. Barone[37], P. Bartalini[22], A. Baschirotto[27], M. Basile[9], R. Battiston[34], A. Bay[22], F. Becattini[16], U. Becker[15], F. Behner[49], J. Berdugo[26], P. Berges[15], B. Bertucci[34], B.L. Betev[49], S. Bhattacharya[10], M. Biasini[34], A. Biland[49], G.M. Bilei[34], R. Bizzarri[37], J.J. Blaising[4], S.C. Blyth[35], G.J. Bobbink[2], R. Bock[1], A. Böhm[1], L. Boldizsar[14], B. Borgia[37], D. Bourilkov[49], M. Bourquin[19], D. Boutigny[4], S. Braccini[19], J.G. Branson[40], V. Brigljevic[49], I.C. Brock[35], A. Buffini[16], A. Buijs[45], J.D. Burger[15], W.J. Burger[34], J. Busenitz[44], X.D. Cai[15], M. Campanelli[49], M. Capell[15], G. Cara Romeo[9], G. Carlino[29], A.M. Cartacci[16], J. Casaus[26], G. Castellini[16], F. Cavallari[37], N. Cavallo[29], C. Cecchi[19], M. Cerrada[26], F. Cesaroni[23], M. Chamizo[26], Y.H. Chang[51], U.K. Chaturvedi[18], S.V. Chekanov[31], M. Chemarin[25], A. Chen[51], G. Chen[7], G.M. Chen[7], H.F. Chen[20], H.S. Chen[7], M. Chen[15], G. Chiefari[29], C.Y. Chien[5], L. Cifarelli[39], F. Cindolo[9], C. Civinini[16], I. Clare[15], R. Clare[15], H.O. Cohn[32], G. Coignet[4], A.P. Colijn[2], N. Colino[26], S. Costantini[8], F. Cotorobai[13], B. de la Cruz[26], A. Csilling[14], T.S. Dai[15], R. D'Alessandro[16], R. de Asmundis[29], A. Degré[4], K. Deiters[47], P. Denes[36], F. DeNotaristefani[37], D. DiBitonto[44], M. Diemoz[37], D. van Dierendonck[2], F. Di Lodovico[49], C. Dionisi[37], M. Dittmar[49], A. Dominguez[40], A. Doria[29], M.T. Dova[18,d], E. Drago[29], D. Duchesneau[4], P. Duinker[2], I. Duran[41], S. Dutta[10], S. Easo[34], Yu. Efremenko[32], H. El Mamouni[25], A. Engler[35], F.J. Eppling[15], F.C. Erné[2], J.P. Ernenwein[25], P. Extermann[19], M. Fabre[47], R. Faccini[37], S. Falciano[37], A. Favara[16], J. Fay[25], O. Fedin[38], M. Felcini[49], B. Fenyi[44], T. Ferguson[35], F. Ferroni[37], H. Fesefeldt[1], E. Fiandrini[34], J.H. Field[19], F. Filthaut[35], P.H. Fisher[15], I. Fisk[40], G. Forconi[15], L. Fredj[19], K. Freudenreich[49], C. Furetta[27], Yu. Galaktionov[28,15], S.N. Ganguli[10], P. Garcia-Abia[6], S.S. Gau[12], S. Gentile[37], J. Gerald[5], N. Gheordanescu[13], S. Giagu[37], S. Goldfarb[22], J. Goldstein[11], Z.F. Gong[20], A. Gougas[5], G. Gratta[33], M.W. Gruenewald[8], V.K. Gupta[36], A. Gurtu[10], L.J. Gutay[46], D. Haas[6], B. Hartmann[1], A. Hasan[30], D. Hatzifotiadou[9], T. Hebbeker[8], A. Hervé[17], J. Hirschfelder[35], W.C. van Hoek[31], H. Hofer[49], H. Hoorani[35], S.R. Hou[51], G. Hu[5], V. Innocente[17], K. Jenkes[1], B.N. Jin[7], L.W. Jones[3], P. de Jong[17], I. Josa-Mutuberria[26], A. Kasser[22], R.A. Khan[18], D. Kamrad[48], Yu. Kamyshkov[32], J.S. Kapustinsky[24], Y. Karyotakis[4], M. Kaur[18,f], M.N. Kienzle-Focacci[19], D. Kim[37], D.H. Kim[43], J.K. Kim[43], S.C. Kim[43], W.W. Kinnison[24], A. Kirkby[33], D. Kirkby[33], J. Kirkby[17], D. Kiss[14], W. Kittel[31], A. Klimentov[15,28], A.C. König[31], A. Kopp[48], I. Korolko[28], V. Koutsenko[15,28], R.W. Kraemer[35], W. Krenz[1], A. Kunin[15,28], P. Lacentre[48,d,e], P. Ladron de Guevara[26], G. Landi[16], C. Lapoint[15], K. Lassila-Perini[49], P. Laurikainen[21], A. Lavorato[39], M. Lebeau[17], A. Lebedev[15], P. Lebrun[25], P. Lecomte[49], P. Lecoq[17], P. Le Coultre[49], H.J. Lee[8], C. Leggett[3], J.M. Le Goff[17], R. Leiste[48], E. Leonardi[37], P. Levtchenko[38], C. Li[20], C.H. Lin[51], W.T. Lin[51], F.L. Linde[2,17], L. Lista[29], Z.A. Liu[7], W. Lohmann[48], E. Longo[37], W. Lu[33], Y.S. Lu[7], K. Lübelsmeyer[1], C. Luci[37], D. Luckey[15], L. Luminari[37], W. Lustermann[47], W.G. Ma[20], M. Maity[10], G. Majumder[10], L. Malgeri[37], A. Malinin[28], C. Maña[26], D. Mangeol[31], S. Mangla[10], P. Marchesini[49], A. Marin[11], J.P. Martin[25], F. Marzano[37], G.G.G. Massaro[2], D. McNally[17], S. Mele[17], L. Merola[29], M. Meschini[16], W.J. Metzger[31], M. von der Mey[1], Y. Mi[22], D. Migani[9], A. Mihul[13], A.J.W. van Mil[31], H. Milcent[17], G. Mirabelli[37], J. Mnich[17], P. Molnar[8], B. Monteleoni[16], R. Moore[3], T. Moulik[10], R. Mount[33], F. Muheim[19], A.J.M. Muijs[2], S. Nahn[15], M. Napolitano[29], F. Nessi-Tedaldi[49], H. Newman[33], T. Niessen[1], A. Nippe[22], A. Nisati[37], H. Nowak[48], Y.D. Oh[43], H. Opitz[1], G. Organtini[37], R. Ostonen[21], S. Palit[12], C. Palomares[26], D. Pandoulas[1], S. Paoletti[37], P. Paolucci[29], H.K. Park[35], I.H. Park[43], G. Pascale[37], G. Passaleva[17], S. Patricelli[29], T. Paul[12], M. Pauluzzi[34], C. Paus[17], F. Pauss[49], D. Peach[17], Y.J. Pei[1], S. Pensotti[27], D. Perret-Gallix[4], B. Petersen[31], S. Petrak[8], A. Pevsner[5], D. Piccolo[29], M. Pieri[16], P.A. Piroué[36], E. Pistolesi[27], V. Plyaskin[28], M. Pohl[49], V. Pojidaev[28,16], H. Postema[15], N. Produit[19], D. Prokofiev[38], J. Quartieri[39], G. Rahal-Callot[49], N. Raja[10], P.G. Rancoita[27], M. Rattaggi[27], G. Raven[40], P. Razis[30], K. Read[32], D. Ren[49], M. Rescigno[37], S. Reucroft[12], T. van Rhee[45], S. Riemann[48], K. Riles[3], O. Rind[3], A. Robohm[49], J. Rodin[15], B.P. Roe[3], L. Romero[26], S. Rosier-Lees[4], Ph. Rosselet[22], W. van Rossum[45], S. Roth[1], J.A. Rubio[17], D. Ruschmeier[8], H. Rykaczewski[49], J. Salicio[17], E. Sanchez[26], M.P. Sanders[31], M.E. Sarakinos[21], S. Sarkar[10], G. Sauvage[4], C. Schäfer[1], V. Schegelsky[38], S. Schmidt-Kaerst[1], D. Schmitz[1], M. Schneegans[4], N. Scholz[49], H. Schopper[50], D.J. Schotanus[31], J. Schwenke[1], G. Schwering[1], C. Sciacca[29], D. Sciarrino[19], L. Servoli[34], S. Shevchenko[33], N. Shivarov[42], V. Shoutko[28], J. Shukla[24], E. Shumilov[28], A. Shvorob[33], T. Siedenburg[1], D. Son[43], V. Soulimov[29], B. Smith[15], P. Spillantini[16], M. Steuer[15], D.P. Stickland[36], H. Stone[36], B. Stoyanov[42], A. Straessner[1], K. Sudhakar[10], G. Sultanov[18], L.Z. Sun[20], G.F. Susinno[19], H. Suter[49], J.D. Swain[18], X.W. Tang[7], L. Tauscher[6], L. Taylor[12], Samuel C.C. Ting[15], S.M. Ting[15],

S.C. Tonwar[10], J. Tóth[14], C. Tully[36], H. Tuchscherer[44], K.L. Tung[7], Y. Uchida[15], J. Ulbricht[49], U. Uwer[17], E. Valente[37], G. Vesztergombi[14], I. Vetlitsky[28], G. Viertel[49], M. Vivargent[4], S. Vlachos[6], R. Völkert[48], H. Vogel[35], H. Vogt[48], I. Vorobiev[17,28], A.A. Vorobyov[38], A. Vorvolakos[30], M. Wadhwa[6], W. Wallraff[1], J.C. Wang[15], X.L. Wang[20], Z.M. Wang[20], A. Weber[1], S.X. Wu[15], S. Wynhoff[1], J. Xu[11], Z.Z. Xu[20], B.Z. Yang[20], C.G. Yang[7], X.Y. Yao[7], J.B. Ye[20], S.C. Yeh[52], J.M. You[35], An. Zalite[38], Yu. Zalite[38], P. Zemp[49], Y. Zeng[1], Z. Zhang[7], Z.P. Zhang[20], B. Zhou[11], Y. Zhou[3], G.Y. Zhu[7], R.Y. Zhu[33], A. Zichichi[9,17,18], F. Ziegler[48]

[1] I. Physikalisches Institut, RWTH, D-52056 Aachen, FRG[a]
III. Physikalisches Institut, RWTH, D-52056 Aachen, FRG[a]
[2] National Institute for High Energy Physics, NIKHEF, and University of Amsterdam, NL-1009 DB Amsterdam, The Netherlands
[3] University of Michigan, Ann Arbor, MI 48109, USA
[4] Laboratoire d'Annecy-le-Vieux de Physique des Particules, LAPP,IN2P3-CNRS, BP 110, F-74941 Annecy-le-Vieux CEDEX, France
[5] Johns Hopkins University, Baltimore, MD 21218, USA
[6] Institute of Physics, University of Basel, CH-4056 Basel, Switzerland
[7] Institute of High Energy Physics, IHEP, 100039 Beijing, China[g]
[8] Humboldt University, D-10099 Berlin, FRG[a]
[9] University of Bologna and INFN-Sezione di Bologna, I-40126 Bologna, Italy
[10] Tata Institute of Fundamental Research, Bombay 400 005, India
[11] Boston University, Boston, MA 02215, USA
[12] Northeastern University, Boston, MA 02115, USA
[13] Institute of Atomic Physics and University of Bucharest, R-76900 Bucharest, Romania
[14] Central Research Institute for Physics of the Hungarian Academy of Sciences, H-1525 Budapest 114, Hungary[b]
[15] Massachusetts Institute of Technology, Cambridge, MA 02139, USA
[16] INFN Sezione di Firenze and University of Florence, I-50125 Florence, Italy
[17] European Laboratory for Particle Physics, CERN, CH-1211 Geneva 23, Switzerland
[18] World Laboratory, FBLJA Project, CH-1211 Geneva 23, Switzerland
[19] University of Geneva, CH-1211 Geneva 4, Switzerland
[20] Chinese University of Science and Technology, USTC, Hefei, Anhui 230 029, China[g]
[21] SEFT, Research Institute for High Energy Physics, P.O. Box 9, SF-00014 Helsinki, Finland
[22] University of Lausanne, CH-1015 Lausanne, Switzerland
[23] INFN-Sezione di Lecce and Universitá Degli Studi di Lecce, I-73100 Lecce, Italy
[24] Los Alamos National Laboratory, Los Alamos, NM 87544, USA
[25] Institut de Physique Nucléaire de Lyon, IN2P3-CNRS,Université Claude Bernard, F-69622 Villeurbanne, France
[26] Centro de Investigaciones Energeticas, Medioambientales y Tecnologicas, CIEMAT, E-28040 Madrid, Spain[c]
[27] INFN-Sezione di Milano, I-20133 Milan, Italy
[28] Institute of Theoretical and Experimental Physics, ITEP, Moscow, Russia
[29] INFN-Sezione di Napoli and University of Naples, I-80125 Naples, Italy
[30] Department of Natural Sciences, University of Cyprus, Nicosia, Cyprus
[31] University of Nijmegen and NIKHEF, NL-6525 ED Nijmegen, The Netherlands
[32] Oak Ridge National Laboratory, Oak Ridge, TN 37831, USA
[33] California Institute of Technology, Pasadena, CA 91125, USA
[34] INFN-Sezione di Perugia and Universitá Degli Studi di Perugia, I-06100 Perugia, Italy
[35] Carnegie Mellon University, Pittsburgh, PA 15213, USA
[36] Princeton University, Princeton, NJ 08544, USA
[37] INFN-Sezione di Roma and University of Rome, "La Sapienza", I-00185 Rome, Italy
[38] Nuclear Physics Institute, St. Petersburg, Russia
[39] University and INFN, Salerno, I-84100 Salerno, Italy
[40] University of California, San Diego, CA 92093, USA
[41] Dept. de Fisica de Particulas Elementales, Univ. de Santiago, E-15706 Santiago de Compostela, Spain
[42] Bulgarian Academy of Sciences, Central Lab. of Mechatronics and Instrumentation, BU-1113 Sofia, Bulgaria
[43] Center for High Energy Physics, Korea Adv. Inst. of Sciences and Technology, 305-701 Taejon, Republic of Korea
[44] University of Alabama, Tuscaloosa, AL 35486, USA
[45] Utrecht University and NIKHEF, NL-3584 CB Utrecht, The Netherlands
[46] Purdue University, West Lafayette, IN 47907, USA
[47] Paul Scherrer Institut, PSI, CH-5232 Villigen, Switzerland
[48] DESY-Institut für Hochenergiephysik, D-15738 Zeuthen, FRG
[49] Eidgenössische Technische Hochschule, ETH Zürich, CH-8093 Zürich, Switzerland
[50] University of Hamburg, D-22761 Hamburg, FRG
[51] National Central University, Chung-Li, Taiwan, China
[52] Department of Physics, National Tsing Hua University, Taiwan, China

Received: 20 February 1998 / Revised version: 23 March 1998 / Published online: 12 August 1998

Abstract. Time-dependent B^0-$\bar{B}^0$ mixing is studied using about two million hadronic Z decays registered by L3 in 1994 and 1995. For this study three techniques are used. Tagging of the b-quark charge at decay time is performed by identifying leptons from semileptonic B decays. The flavour of the b quark at production time is determined from the charge of the lepton in the opposite hemisphere or by using a jet-charge technique. The proper time of the B-particle decay is obtained by reconstructing the production and decay vertices or by a measurement of the lepton impact parameter. The combined result for the frequency of B_d^0 meson oscillations is

$$\Delta m_d = 0.444 \pm 0.040 \text{ ps}^{-1}.$$

Introduction

As in the case of K mesons, oscillations between particle and antiparticle states are expected in the system of neutral B mesons. In the Standard Model [1], the mechanism causing mixing is a second order weak interaction through box diagrams. The flavour eigenstates B_d^0 ($\bar{b}d$) and $\bar{B}_d^0$ ($b\bar{d}$) are linear combinations of the mass eigenstates B_1 and B_2. Neglecting effects from CP violation (expected to be small), the probability to find a B_d^0 decaying at proper time t, provided it was produced as $\bar{B}_d^0$ at $t = 0$, is given by

$$P(\bar{B}_d^0 \to B_d^0) = \frac{1}{\tau} e^{-\frac{t}{\tau}} \left(\frac{1 - \cos \Delta m_d t}{2} \right)$$

where τ is the lifetime of the B_d^0-meson. A measurement of the oscillation frequency thus gives a direct measurement of the mass difference Δm_d between the two mass eigenstates.

The phenomenon of B^0-$\bar{B}^0$ mixing is well established by experiment [2–4]. The time dependence of mixing for B_d^0 mesons has been measured at LEP, SLC and at the Tevatron using different techniques [5–10].

We present here a measurement of the B_d^0 oscillation frequency with the L3 detector. Three methods — dilepton decay length, lepton – jet charge and dilepton impact parameter — are used for this study. In the dilepton method we use leptons in opposite hemispheres to tag the flavour of the B particle at production and decay time. In the lepton – jet charge method the lepton tags the state of the B particle at the instant of its decay, and the flavour of the primordial b quark is determined using a jet-charge technique. The signature for mixing is the presence of a same-sign lepton pair or a same-sign lepton – jet charge combination. Proper time is measured by reconstructing secondary vertices or using lepton impact parameter information. We combine the three individual measurements. The event sample corresponds to about two million hadronic Z decays recorded in 1994 and 1995.

The L3 detector

The L3 detector is described in detail in [11]. It consists of a central tracking chamber, a high-resolution electromagnetic calorimeter composed of bismuth germanium oxide (BGO) crystals, a ring of plastic scintillation counters, a uranium and brass hadron calorimeter with proportional wire chamber readout and a high resolution muon chamber system. These detectors are installed in a 12 m diameter magnet which provides a uniform field of 0.5 T along the beam direction.

The muon spectrometer, located outside the hadron calorimeter, consists of three layers of drift chambers which measure 56 points on the muon trajectory in the bending plane (r-ϕ) and 8 points in the non-bending direction (z).

The material preceding the barrel part of the electromagnetic calorimeter amounts to less than 10% of a radiation length. In this region the energy resolution of the BGO calorimeter is better than 2% and the angular resolution of electromagnetic clusters is better than 0.5° for energies above 1 GeV.

The central tracking chamber is a time expansion chamber (TEC) which consists of two cylindrical layers of 12 and 24 sectors, with a total of 62 wires measuring r-ϕ coordinates. The single wire resolution ranges from 35 μm to 100 μm depending on the drift distance. A chamber mounted just outside the TEC provides z coordinate measurements.

A Silicon Microvertex Detector (SMD) was installed inside the L3 detector during 1993. It consists of two cylindrical layers of double-sided silicon microstrip detectors, placed at 6 cm and 8 cm from the beam axis, respectively, covering $\approx 90\%$ of the solid angle. Each layer consists of 12 basic modules, constructed out of four silicon sensors 70 mm long, 40 mm wide and 300 μm thick, with a readout pitch of 50 μm on the junction (r-ϕ) side and 150/200 μm on the ohmic (z) side. The intrinsic resolution of the SMD is 7 μm on the junction side and 15 μm on the ohmic side [12].

[a] Supported by the German Bundesministerium für Bildung, Wissenschaft, Forschung und Technologie
[b] Supported by the Hungarian OTKA fund under contract numbers T14459, T19181 and T24011
[c] Supported also by the Comisión Interministerial de Ciencia y Tecnología
[d] Also supported by CONICET and Universidad Nacional de La Plata, CC 67, 1900 La Plata, Argentina
[e] Supported by Deutscher Akademischer Austauschdienst
[f] Also supported by Panjab University, Chandigarh-160014, India
[g] Supported by the National Natural Science Foundation of China

Tracks are first reconstructed in the TEC. They are then extrapolated to the SMD layers and refitted using the matched SMD hits.

Dilepton decay length method

The published dilepton analysis [8] is extended here to include the data taken in 1995.

Tagging of the b-quark charge at decay time is performed by identifying leptons from semileptonic B decays. The flavour of the b quark at production time is determined from the charge of the lepton in the opposite hemisphere. The selected leptons (electrons or muons) must have a high momentum and a high transverse momentum with respect to the closest jet direction.

To estimate the decay length of a b-hadron candidate we reconstruct the primary and secondary vertex positions. Vertex finding is performed in the r-ϕ plane perpendicular to the beam axis. The direction of the jet containing the lepton is then used to obtain a three-dimensional decay length. To calculate the proper time, one needs to know the momentum of the b-hadron. A constant fraction of the beam energy is used for this momentum estimate. The value $p_B = 0.85\ E_{beam}$ is found to optimize the proper time resolution. The JETSET 7.4 Monte Carlo program [13] is used to generate hadronic Z decays. The detector simulation is performed with a GEANT-based description of the L3 detector [14].

For the fit of the B^0_d-$\bar{B}^0_d$ oscillation frequency dilepton events with at least one proper time measured are selected. 1490 dilepton events with 1928 secondary vertices fulfill all requirements of lepton identification and vertex reconstruction. There are 630 reconstructed vertices in the like-sign events and 1298 in the unlike-sign ones.

An eight-parameter unbinned maximum-likelihood fit is performed in order to determine Δm_d. A likelihood is assigned to each event proportional to the probability density to find such an event at the measured decay time. Fitted parameters are Δm_d itself and f_{Λ_b}, f_s, F_{bcl}, where f_{Λ_b} and f_s are the fractions of b-baryons and B_s mesons in the sample, and F_{bcl} is the fraction of leptons coming from cascade decays ($b \to c \to \ell$, $b \to \bar{c} \to \ell$, $b \to J \to \ell^+\ell^-$) in $\bar{b}$ events. The other four parameters are the lifetimes of b-hadrons: τ_d for B^0_d, τ_u for B_u, τ_s for B_s and τ_{Λ_b} for Λ_b. The oscillation frequency Δm_d is a free parameter; for the other seven parameters Gaussian constraints are applied with the central values and errors quoted in Table 1. The value for the B_s fraction in $\bar{b}$ events (f_s) is fixed to the world average derived from time-integrated mixing measurements and D_s-lepton correlations [15]. The value for the fraction of b-baryons in $\bar{b}$ events is derived from Λ_c-lepton and Λ-lepton correlations [16]. The fractions of B^0_d and B_u are then obtained through $f_d = f_u = 0.5 \times (1 - f_{\Lambda_b} - f_s)$. The central values and uncertainties of the b-hadron lifetimes are taken from [17]. We also impose a Gaussian constraint on the mean lifetime of the b-hadrons, $\tau_b = f_d\tau_d + f_u\tau_u + f_s\tau_s + f_{\Lambda_b}\tau_{\Lambda_b}$, requiring it to be compatible with the world average value $\tau_b = 1.549 \pm 0.020$ ps [17].

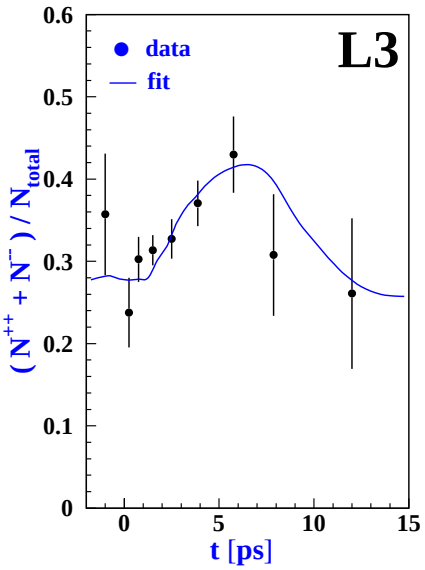

Fig. 1. Ratio of the number of same-sign dilepton events to the total number of dilepton events versus the measured proper time compared to the fit result (solid line)

The result of the fit is $\Delta m_d = 0.458 \pm 0.054$ ps^{-1}. The error on Δm_d includes the statistical error as well as a contribution from systematic errors of the constrained parameters. To separate out the statistical error we fix all the constrained parameters to their fitted values and perform a one-parameter fit. This gives $\Delta m_d = 0.458 \pm 0.046$ (stat) ps^{-1} where the error is purely statistical. The systematic error on Δm_d is then obtained by subtracting in quadrature the statistical error from the eight-parameter fit error. This gives ± 0.028 ps^{-1} for the systematic error estimate. The individual systematic errors on Δm_d from fitted parameters are estimated by shifting the central value of each constrained parameter by the uncertainty quoted in Table 1 and refitting. The change in Δm_d is taken as systematic error. Due to correlations, the sum in quadrature of the contributions obtained this way is not equal to the total systematic error above (labelled "subtotal" in Table 1). Therefore the individual systematic errors on Δm_d from fitted parameters are scaled to add up in quadrature to 0.028 ps^{-1}.

The values of other parameters are the same as in the 1994 data analysis [8]. The contributions to the systematic error on Δm_d are summarized in Table 1. The fraction of like-sign leptons is plotted in Fig. 1 as a function of proper time and compared to the fit result.

The oscillation frequency is found to be

$$\Delta m_d = 0.458 \pm 0.046(\text{stat}) \pm 0.032(\text{syst})\ \text{ps}^{-1}$$

by the dilepton decay length method.

Lepton – jet charge method

As in the dilepton method described above, the state of the B meson at the instant of its decay is tagged by the

Table 1. Summary of contributions to the systematic error on Δm_d using the dilepton decay length method. $F^{\rm MC}_{bcl}$ is the relative fraction of cascade decays derived from the MC simulation [13,14]

Parameter	Input / Variation	Fitted value	$\Delta(\Delta m_d)$ [ps^{-1}]
Λ_b fraction (f_{Λ_b})	0.087 ± 0.029	0.086 ± 0.027	± 0.007
B_s fraction (f_s)	0.102 ± 0.016	0.104 ± 0.015	∓ 0.015
cascade decay fraction (F_{bcl})	$F^{\rm MC}_{bcl}\,(1. \pm 0.15)$	$F^{\rm MC}_{bcl}\,(1.04 \pm 0.13)$	∓ 0.022
τ_d	1.56 ± 0.06 ps	1.57 ± 0.05 ps	∓ 0.003
τ_u	1.62 ± 0.06 ps	1.64 ± 0.05 ps	± 0.006
τ_s	1.61 ± 0.10 ps	1.61 ± 0.10 ps	± 0.001
τ_{Λ_b}	1.14 ± 0.08 ps	1.12 ± 0.08 ps	± 0.001
τ_b	1.549 ± 0.020 ps	—	∓ 0.002
subtotal	—	—	0.028
fakes fraction (F_{bfk})	$\pm 30\%$	—	∓ 0.007
$c\bar{c}$ fraction (f_c)	$\pm 30\%$	—	± 0.001
uds fraction (f_{uds})	$\pm 50\%$	—	∓ 0.001
resolution	$\pm 25\%$	—	± 0.007
boost term	see [8]	—	± 0.006
w_{bl}	$\pm 30\%$	—	∓ 0.003
w_{bcl}	± 0.05	—	∓ 0.007
w_{bfk}	± 0.10	—	∓ 0.006
w_{udsc}	± 0.10	—	∓ 0.001
Δm_s	3 – 20 ps^{-1}	—	∓ 0.001
total			0.032

lepton that originates from its semileptonic decay. The lepton must pass the selection criteria applied in the dilepton method. The decay time of the b-hadron is also reconstructed in the same way. Although the reconstruction of a secondary vertex in the hemisphere that does not contain the lepton (the *opposite* hemisphere) would not be necessary for this analysis, requiring it increases the b-purity of the sample from 91% to 97%.

The B meson's state at the time of its production is tagged using jet charges, as the spatial distribution of charge in the event tends to reflect the orientation of the primordial quark–antiquark pair. A jet charge is calculated as a weighted sum of charges in a hemisphere defined by the thrust axis:

$$Q_{jet} = \frac{\sum_i w_i q_i}{\sum_i w_i} \quad \text{with} \quad w_i = C_i\, p_{iL}^{\kappa}\ , \qquad (1)$$

where q_i is the charge of the ith track in the hemisphere and its weight, w_i, is proportional to a power of the longitudinal component of the track's momentum with respect to the thrust axis, p_{iL}. Coefficient C_i is the probability of correct track charge assignment. Since this probability decreases as the track passes nearer to the anode wire plane in the TEC, C_i depends on the azimuthal angle: $C_i = C(\phi_i)$. Function $C(\phi_i)$ is determined by studying Bhabha events. The power κ is found in Monte Carlo studies by maximizing the probability of reconstructing the correct jet charge. The maximum is found at $\kappa = 0.4$. Monte Carlo studies show that in the lepton's hemisphere the value of jet charge depends on whether the B meson changed flavour (mixed event) or not. In order to decrease

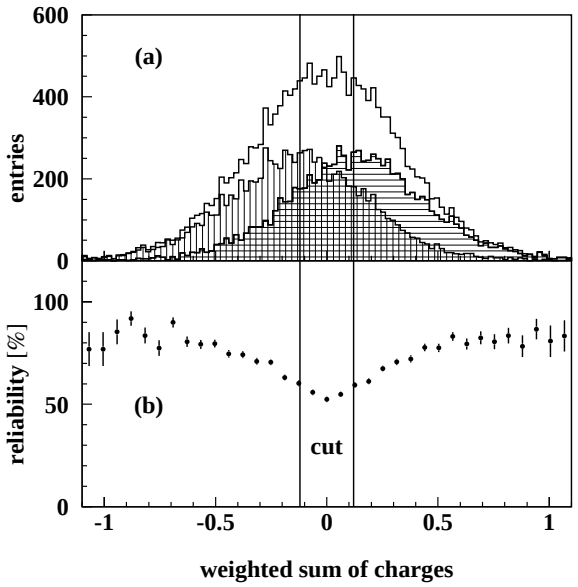

Fig. 2. **a** $Q = Q^{\kappa=0.4}_{opp} - Q^{\kappa=0}_{lepton}$ for a b-quark jet (*horizontally hatched histogram*) and a b-quark jet (*vertically hatched histogram*) as determined by Monte Carlo. The unhatched histogram is their sum, **b** the probability of correct jet charge reconstruction (reliability) as a function of Q. This probability tends to 50% at $Q = 0$ so the power of separation vanishes there. The two vertical lines delimit the excluded low reliability interval

this correlation, we set $\kappa = 0$ in the lepton's hemisphere. Thus the tagging variable is $Q = Q_{opp}^{\kappa=0.4} - Q_{lepton}^{\kappa=0}$, where $Q_{opp}^{\kappa=0.4}$ is the jet charge of the *opposite* hemisphere calculated according to (1) using $\kappa = 0.4$, and $Q_{lepton}^{\kappa=0}$ is the jet charge of the hemisphere containing the lepton, calculated using $\kappa = 0$. Figure 2 shows the distribution of Q for a b-quark jet and a $\bar{\text{b}}$-quark jet.

To be included in the jet charge sum calculation, a track must have a momentum in the r-ϕ plane greater than 0.5 GeV, at least 10 TEC hits with a span of at least 20 wires[1], and a distance of closest approach to the average position of the e^+e^- collision point in the r-ϕ plane less than 20 mm.

To increase the tagging power of the method, events with $|Q| < 0.12$ are rejected. This way the region of low reliability (probability for correct charge reconstruction) is excluded (see Fig. 2). The reliability is found to be 72% for unmixed events and 67% for mixed events. The number of events passing all selection criteria is 8707.

In order to extract the oscillation frequency, an unbinned maximum-likelihood fit is performed. Each event is assigned a likelihood depending on whether it exhibits a like or unlike signed lepton – jet charge combination as function of the lepton proper time:

$$\begin{aligned}\mathcal{L}_{like}(t) = &\sum_{i\in\{mix,\ unmix\}} [R^i(t)(1-P^i) + W^i(t)P^i] \\ &+ \sum_{i\in\{c,\ uds\}} f_i w_i Z_i(t)\ , \\ \mathcal{L}_{unlike}(t) = &\sum_{i\in\{mix,\ unmix\}} [R^i(t)P^i + W^i(t)(1-P^i)] \\ &+ \sum_{i\in\{c,\ uds\}} f_i (1-w_i) Z_i(t)\ ,\end{aligned}$$

where P^{mix} (P^{unmix}) is the reliability of the jet charge reconstruction in b-flavoured events with (without) mixing. $Z_c(t)$ and $Z_{uds}(t)$ are the reconstructed decay time distributions of Monte Carlo c-flavoured (fraction f_c) and light-quark events (fraction f_{uds}), and w_c and w_{uds} denote the probabilities of like-sign combination in c-flavoured and light-flavoured events. $R^{mix}(t)$ and $R^{unmix}(t)$ are the probabilities to find, at proper time t, a lepton with the "right" sign of charge (the sign expected from the primordial quark decay without mixing) in a mixed or unmixed event, respectively. They are expressed as

$$\begin{aligned}R^{mix}(t) = &\sum_{j\in\{bl,\ bcl,\ bfk\}} F_j w_j M(t)\ , \\ R^{unmix}(t) = &\sum_{j\in\{bl,\ bcl,\ bfk\}} F_j (1-w_j)(D(t) - M(t))\ . \quad (2)\end{aligned}$$

F_{bl}, F_{bcl} and F_{bfk} are the fractions of the various types of $\bar{\text{b}}$ events: leptons coming from semileptonic decays of b-hadrons, cascade decays and fake leptons in $\bar{\text{b}}$ events, respectively. The w factors (w_{bl}, w_{bcl} and w_{bfk}) give the probabilities to find a lepton sign opposite to the one expected if the event resulted from an unmixed B decay. The "wrong" sign probabilities $W^{mix}(t)$ and $W^{unmix}(t)$ are obtained from 2 by exchanging w_j and $(1-w_j)$. $M(t)$ is the probability of a mixed B meson to decay at a reconstructed time t while $D(t)$ is that of any b-hadron to decay at a reconstructed time t:

$$\begin{aligned}M(t) = &\sum_{m\in\{d,\ s\}} f_m \int_0^\infty \frac{\epsilon(t')}{N_m}\,\frac{1}{\tau_m}\, e^{-\frac{t'}{\tau_m}} \\ &\times \frac{1-\cos \Delta m_m t'}{2}\, U(t,t')\, dt'\ , \\ D(t) = &\sum_{n\in\{u,\ d,\ s,\ \Lambda_b\}} f_n \int_0^\infty \frac{\epsilon(t')}{N_n}\,\frac{1}{\tau_n}\, e^{-\frac{t'}{\tau_n}}\, U(t,t')\, dt'\ .\end{aligned}$$

The resolution function $U(t,t')$ is described in [8]. The oscillation frequency Δm_s of B_s mesons was fixed to 10 ps^{-1}, thus assuming a large mixing in the B_s system. $\epsilon(t)$ stands for the efficiency of proper time reconstruction and the normalization factors N_i ($i \in \{d, s, u, \Lambda_b\}$) are defined by the requirements

$$\int_{-\infty}^{\infty} dt \int_0^\infty dt'\ \frac{\epsilon(t')}{N_i}\,\frac{1}{\tau_i}\, e^{-\frac{t'}{\tau_i}}\, U(t,t') = 1\ . \qquad (3)$$

Nine parameters are allowed to vary in the fit to the data sample. Δm_d and P^{unmix} are free whereas Gaussian constraints are imposed upon P^{mix}, τ_d, τ_u, τ_s, τ_{Λ_b}, f_{Λ_b} and f_s. The average b-hadron lifetime is constrained as in the dilepton fit. The central value of P^{mix} is set to its Monte Carlo value. Its uncertainty is estimated as follows: we fit data with $Q_{opp}^{\kappa=0.4}$ taken as the tagging variable. This fit yields for the reliability of the jet charge reconstruction in the *opposite* hemisphere $P_{opp} = 0.634 \pm 0.012$ whereas the Monte Carlo value is $P_{opp}^{MC} = 0.660 \pm 0.005$. The difference between them is used as an estimate of the uncertainty on P^{mix}.

The result of the fit is $\Delta m_d = 0.437 \pm 0.060$ ps^{-1}. Treating the errors in the same fashion as in the dilepton analysis, we obtain

$$\Delta m_d = 0.437 \pm 0.043\ (\text{stat}) \pm 0.044\ (\text{syst})\ \text{ps}^{-1}\ .$$

The contributions to the systematic error on Δm_d coming from individual parameters are itemized in Table 2. The like-sign fraction is plotted in Fig. 3 as a function of proper time together with the result of the fit.

Dilepton impact parameter method

A third determination of neutral B mixing is based on measured impact parameters of leptons in dilepton events. In this method the time of decay is measured indirectly and statistically from the impact parameters of the reconstructed lepton trajectories with respect to the beam axis. This method has the advantage of permitting less stringent selection requirements on the b candidates, thereby

[1] The span is the distance between the first and the last hit in units of the wire spacing

Table 2. Summary of contributions to the systematic error on Δm_d using the lepton – jet charge method. $F^{\rm MC}_{bcl}$ is the relative fraction of cascade decays derived from the MC simulation [13,14]

Parameter	Input / Variation	Fitted value	$\Delta(\Delta m_d)$ [ps^{-1}]
P^{unmix}	free	0.733 ± 0.011	± 0.037
P^{mix}	0.670 ± 0.030	0.679 ± 0.029	∓ 0.015
Λ_b fraction (f_{Λ_b})	0.087 ± 0.029	0.089 ± 0.025	± 0.004
B_s fraction (f_s)	0.102 ± 0.016	0.101 ± 0.016	± 0.001
τ_d	1.56 ± 0.06 ps	1.60 ± 0.05 ps	∓ 0.002
τ_u	1.62 ± 0.06 ps	1.64 ± 0.05 ps	± 0.004
τ_s	1.61 ± 0.10 ps	1.63 ± 0.10 ps	± 0.002
τ_{Λ_b}	1.14 ± 0.08 ps	1.11 ± 0.08 ps	± 0.002
τ_b	1.549 ± 0.020 ps	—	∓ 0.001
subtotal	—	—	0.041
cascade decay fraction (F_{bcl})	$F^{\rm MC}_{bcl}$ $(1. \pm 0.15)$		± 0.002
fakes fraction (F_{bfk})	$\pm 30\%$	—	± 0.001
$c\bar{c}$ fraction (f_c)	$\pm 30\%$	—	± 0.001
uds fraction (f_{uds})	$\pm 50\%$	—	± 0.002
resolution	$\pm 25\%$	—	± 0.009
boost term	see [8]	—	± 0.006
w_{bl}	$\pm 30\%$	—	± 0.001
w_{bcl}	± 0.05	—	± 0.001
w_{bfk}	± 0.10	—	± 0.001
w_c	± 0.10	—	∓ 0.002
w_{uds}	± 0.10	—	± 0.004
Δm_s	3 – 20 ps^{-1}	—	$+0.004$
total			0.044

Table 3. Summary of contributions to the systematic error on Δm_d using the dilepton impact parameter method. The wrong-sign probabilities $w_{b\ell}$ and $w_{bc\ell}$ refer solely to the contributions from tracking charge confusion. w_{bkg} is the w factor for background from light-quark events and from fake leptons in $b\bar{b}$ events

Parameter	Input / Variation	Fitted value	$\Delta(\Delta m_d)$ [ps^{-1}]
Λ_b fraction (f_{Λ_b})	0.117 ± 0.034	0.112 ± 0.034	± 0.015
B_s fraction (f_s)	0.102 ± 0.016	0.102 ± 0.015	∓ 0.026
$b \to c \to \ell$ fraction	0.080 ± 0.012	0.083 ± 0.011	∓ 0.037
subtotal	–	–	0.048
fakes fraction	$(4.6 \pm 1.3)\%$	–	$\mp$ 0.011
$c\bar{c}$ fraction	$(1.5 \pm 0.3)\%$	–	$\pm$ 0.001
$b \to \bar{c} \to \ell$ fraction	$(1.0 \pm 0.3)\%$	–	$\pm$ 0.001
τ_d	1.56 ± 0.06 ps	–	$\mp$ 0.017
τ_s	1.61 ± 0.10 ps	–	$\mp$ 0.002
τ_b	1.549 ± 0.020 ps	–	$\pm$ 0.002
b fragmentation: $\langle x \rangle$	0.72 ± 0.02	–	$\pm$ 0.002
resolution function	–	–	$\pm$ 0.001
$w_{b\ell}$	$(0.24 \pm 0.02)\%$	–	$\mp$ 0.001
$w_{bc\ell}$	$(0.24 \pm 0.02)\%$	–	$\pm$ 0.000
w_{bkg}	$(33.7 \pm 3.4)\%$	–	$\mp$ 0.008
w_c	$(10.0 \pm 3.0)\%$	–	$\mp$ 0.002
Δm_s	5 – 25 ps^{-1}	–	$-$ 0.004 $+$ 0.008
total			0.053

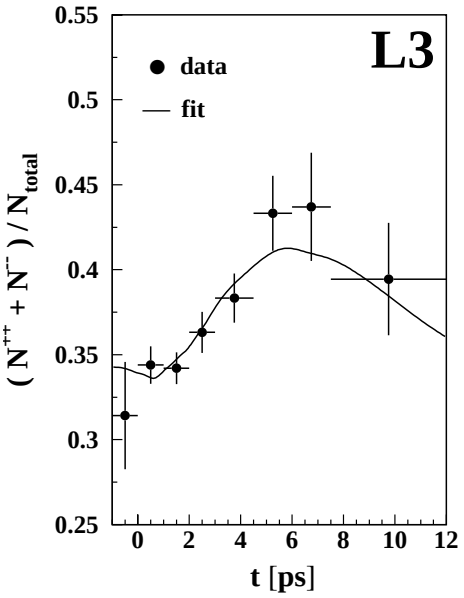

Fig. 3. The ratio of the number of like-sign events as determined by jet charge and lepton to the total number of events as a function of the measured proper time. The solid line is the result of the fit

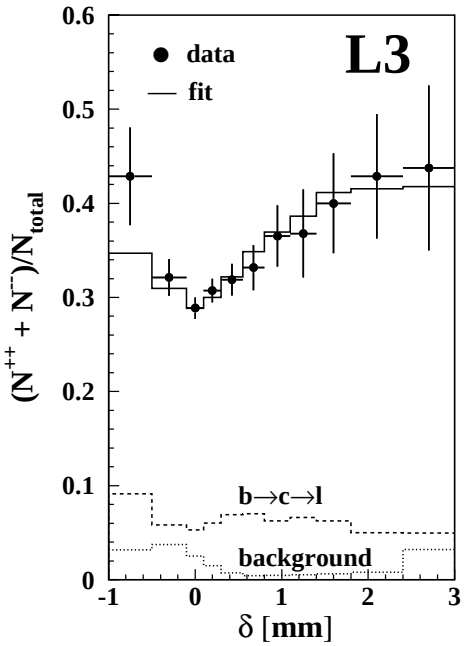

Fig. 4. Ratio of the number of same-sign dilepton events to the total number of dilepton events as a function of δ (the measured impact parameter) compared to the fit result. The individual contributions to the distribution from cascade decays ($b \to c \to \ell$) and background leptons (misidentified hadrons) are shown by dashed and dotted lines, respectively

increasing statistics. Systematic uncertainties, however, are larger using the impact parameter method due to lower b-purity of the selected event sample.

Event selection requirements for the impact parameter method are nearly identical to those used for the decay length method, except that no primary or secondary vertex requirements are imposed on either candidate b-jet. The ratio of the number of same-sign dilepton events to the total number of dilepton events as a function of δ, the measured impact parameter, is plotted in Fig. 4. The selected event sample consists of 2596 dilepton events.

A simultaneous, binned, maximum-likelihood fit to the like- and opposite-sign impact parameter distributions determines the oscillation frequency Δm_d. Again values are assumed for parameters such as f_d, f_s and Δm_s, and multi-parameter fits are performed to verify the consistency of these assumed parameter values with the observed data. The like-sign and opposite-sign distributions in the data are fitted to predictions from reweighted Monte Carlo events. For each event in the data, the likelihood contribution is a sum of products of right- and wrong-sign probabilities for the two measured impact parameter bins, where the combination of products used depends on whether the leptons signs are same- or opposite-sign. Reweighting affects composition fractions and right- and wrong-sign probabilities for both signal and background events. Monte Carlo impact parameter resolutions are not used. Instead, the resolutions are determined directly from data, using control samples of hadronic tracks chosen geometrically to have preferentially small true impact parameters in the plane transverse to the beam axis. All control tracks must satisfy identical tracking quality requirements of the lepton candidates. They must also satisfy the same requirement of transverse momentum with respect to the associated jet. Reweighting corrections are applied to the control samples to reproduce kinematic, geometrical, and isolation characteristics of the leptons in the dilepton sample before resolution functions are extracted [18]. These characteristics include binned distributions in azimuth angle with respect to the beam direction, transverse momentum with respect to the jet, track curvature, number and span of tracking chamber hits, and nearness to anode and cathode wire planes in the TEC. The resolution functions for electrons and muons are parametrized as sums of three Gaussian corrections to the impact parameter error obtained from the original track fit [19].

From the resolution functions and the underlying true impact parameter distributions for hadronic Z decays as obtained from Monte Carlo, one can also predict the expected impact parameter distributions for single-lepton candidates satisfying the electron and muon selection requirements. Comparison of the observed and expected impact parameter distributions shows good qualitative agreement between data and Monte Carlo. As a quantitative test, a fit has been performed to obtain the mean b-hadron lifetime. Values consistent with the L3 measurement of the b lifetime [20] are obtained for single electron and single muon samples in both 1994 and 1995.

Systematic uncertainties arising in the impact parameter method are estimated in a similar way as for the decay length method. Results are summarized in Table 3.

The result for Δm_d using the dilepton impact parameter method is

$$\Delta m_d = 0.472 \pm 0.049(\text{stat}) \pm 0.053(\text{syst}) \text{ ps}^{-1}.$$

Combination of Δm_d results

In order to combine individual results quoted above we measure Δm_d on statistically independent samples. The dilepton decay length event sample is left untouched and the other two event samples are reduced to eliminate statistical overlap. The fit was redone on the two reduced samples and the new central values and statistical errors are used in the combination procedure. A combination of the results is done in a global χ^2 fit which takes into account correlations from common sources of systematics. The systematic uncertainties from b-hadron fractions, B lifetimes, cascade decay fractions, B momentum and charge confusion (w factors in Tables 1, 2 and 3) are assumed to be fully correlated. Uncertainties from resolution are also considered correlated for the dilepton decay length and lepton – jet charge methods. The set of input parameters used in the fit for the dilepton decay length and lepton – jet charge methods is the same (Table 1 and 2). Parameter values in the dilepton impact parameter measurement and their errors are adjusted to agree with the ones used in the other methods.

The combined result for Δm_d is then

$$\begin{aligned}\Delta m_d &= 0.444 \pm 0.028 \pm 0.028 \text{ ps}^{-1} \\ &= (2.92 \pm 0.18 \pm 0.18)\ 10^{-4} \text{ eV} .\end{aligned}$$

This improves and supersedes the previous L3 result on Δm_d . The result is also consistent with the current world average $\Delta m_d = 0.474 \pm 0.031$ ps^{-1} [17].

Acknowledgements. We wish to express our gratitude to the CERN accelerator divisions for the excellent performance of the LEP machine. We also acknowledge and appreciate the effort of the all engineers, technicians and support staff who have participated in the construction and maintenance of this experiment.

References

1. S.L. Glashow, Nucl. Phys. **22** (1961) 579; S. Weinberg, Phys. Rev. Lett. **19** (1967) 1264; A. Salam, "Elementary Particle Theory", Ed. N. Svartholm, Stockholm, "Almquist and Wiksell" (1968), 367
2. UA1 Collaboration, C. Albajar et al., Phys. Lett. **B 186** (1987) 247
3. ARGUS Collaboration, H. Albrecht et al., Phys. Lett. **B 192** (1987) 245; ARGUS Collaboration, H. Albrecht et al., Phys. Lett. **B 324** (1994) 249; CLEO Collaboration, J. Bartelt et al., Phys. Rev. Lett. **71** (1993) 1680
4. ALEPH Collaboration, D. Buskulic et al., Phys. Lett. **B 284** (1992) 177; DELPHI Collaboration, P. Abreu et al., Phys. Lett. **B 332** (1994) 488; L3 Collaboration, M. Acciarri et al., Phys. Lett. **B 335** (1994) 542; OPAL Collaboration, R. Akers et al., Z. Phys. **C 60** (1993) 199
5. ALEPH Collaboration, D. Buskulic et al., Z. Phys. **C 75** (1997) 397
6. CDF Collaboration, F. Abe et al., FERMILAB-PUB-97/312-E, to be published in Phys. Rev. Lett.
7. DELPHI Collaboration, P. Abreu et al., Z. Phys. **C 76** (1997) 579
8. L3 Collaboration, M. Acciarri et al., Phys. Lett. **B 383** (1996) 487
9. OPAL Collaboration, G. Alexander et al., Z. Phys. **C 72** (1996) 377; OPAL Collaboration, K. Ackerstaff et al., Z. Phys. **C 76** (1997) 401; OPAL Collaboration, K. Ackerstaff et al., Z. Phys. **C 76** (1997) 417
10. SLD Collaboration SLAC-PUB-7228, contributed paper PA08-026A to ICHEP'96 Warsaw; SLD Collaboration SLAC-PUB-7229, contributed paper PA08-026B to ICHEP'96 Warsaw; SLD Collaboration SLAC-PUB-7230, contributed paper PA08-026C to ICHEP'96 Warsaw
11. L3 Collaboration, B. Adeva et al., Nucl. Instr. and Meth. **A 289** (1990) 35; L3 Collaboration, O. Adriani et al., Phys. Rep. **236** (1993) 1
12. M. Acciarri et al., Nucl. Instr. and Meth. **A 351** (1994) 300
13. T. Sjöstrand, Comput. Phys. Commun. **39** (1986) 347; T. Sjöstrand and M. Bengtsson, Comput. Phys. Commun. **43** (1987) 367
14. The L3 detector simulation is based on GEANT Version 3.14; see R. Brun et al., GEANT 3, CERN DD/EE/84-1 (Revised), September 1987 and the GHEISHA program (H. Fesefeld, RWTH Aachen Report PITHA85/02 (1985)) for the simulation of hadronic interactions
15. S.L. Wu, "Recent Results on B Meson Oscillations", Proc. of Int. Symp. on Lepton-Photon Interactions, Beijing, China (August 1995), Z.P. Zheng and H.S. Chen *eds* (World Scientific)
16. DELPHI Collaboration, P. Abreu et al., Z. Phys. **C 74** (1997) 19
17. Particle Data Group, Phys. Rev. **D 54** (1996) 1
18. Y. Zhou, "Measurement of $B_d^0\bar{B}_d^0$ Oscillation Frequency Using Dilepton Events", Ph.D. thesis, University of Michigan, June 1997
19. L3 Collaboration, B. Adeva et al., Phys. Lett. **B 270** (1991) 111; L3 Collaboration, O. Adriani et al., Phys. Lett. **B 317** (1993) 474
20. L3 Collaboration, M. Acciarri et al., Phys. Lett. **B 416** (1997) 220